AFPM Machines Equipped with Multilayer Magnets

Mostafa Ahmadi Darmani, *Member*, *IEEE*, Emir Pošković, *Member, IEEE*, Fausto Franchini,
Luca Ferraris, *Member, IEEE*, Andrea Cavagnino, *Fellow, IEEE,* and Chris Gerada, *Senior Member, IEEE*

Abstract—**This article investigates the manufacturability and applicability of unified multilayer magnets, comprising two different magnetic materials with distinct characteristics, for use in electrical machines. In particular, the self-produced multilayer magnets are made of compressed NdFeB bonded powders for the '*strong*' magnet layer and hybrid composite materials for the '*weak*' magnet layer. Various combinations of material for the self-produced permanent magnets are experimentally investigated. Also, the suitability of resultant multilayer bonded magnets to electrical machines is articulated on the basis of finite element simulations. To assess their performance, three axial-flux surface-mounted permanent magnet machines are constructed: one conventional machine with single-layer bonded magnets as the reference, and two machines equipped with multilayer magnets with series and parallel configurations. The performance of the machines are evaluated in terms of the back-EMF, output torque, torque ripple, losses, efficiency, and cost. The findings indicate an appreciable enhancement in flux-weakening operation for the machine equipped with multilayer magnets, but at the expense of lower flux linkage values and nominal torque. Further analyses of the multilayer magnet's trade-offs and potential applications in electrical machines are presented.**

Index Terms—**Multilayer permanent magnets, synchronous PM machines, axial flux machines, bonded magnets, hybrid magnets, high efficiency, variable flux machines, flux weakening, cost-efficient, FEM simulations.**

I. INTRODUCTION

PERMANENT magnet (PM) synchronous machines are extensively exploited in numerous applications because of their high power and torque density, as well as for their high-efficiency values in a wide range of rotational speeds. However, the magnetisation field generated by the magnets is intrinsically constant. This principle can cause some challenges during the machine's operation, specifically at high speed. In this condition, the induced back Electro-Motive Force (EMF) increases and can reach the maximum defined voltage limit of the drive. Furthermore, the large flux density values, together with the high supply frequencies required at high rotational speed, lead to considerable losses in the laminations and windings. However,

dedicated flux-weakening control techniques can also allow constant power speed range regulation for machines equipped with permanent magnets. To respect the voltage constraints, a part of the current flowing in the stator windings is utilised to generate a magnetic field in the opposite direction to that of PMs. In other words, this current component is just used to partially demagnetise the magnets, and it does not contribute to the torque production. However, this additional current component leads to a significant increase in copper Joule losses and core losses due to the harmonics of the flux density [1]. Several solutions have been proposed to enhance the flux weakening capability of the machine taking into consideration additional excitation windings or dedicated PM topologies. For instance, hybrid excitation machines technologies take advantage of wound field excitation and PMs, improving the machine operation at flux weakening operation. In this way, the *dc* coils, which can be placed '*in series*' or '*in parallel*' to the magnets, are taken into account to adjust the air gap flux density [2], [3]. Nevertheless, it seems that it is not an efficient solution for high-speed applications since the *dc* winding introduces additional Joule losses. Besides, this structure requires to supply rotating coils, which is quite challenging.

Recently, flux memory machines and variable flux synchronous machines have been presented as alternative solutions. In these machine topologies, the value of air gap flux density can be manipulated by injecting large current pulses through the stator windings [4]–[7]. In detail, the pulse current component is injected in the negative direction of d-axis to partially demagnetise the magnets without taking into account extra circuits and continuous flowing of high currents. Nevertheless, this solution requires a precise control strategy and detailed information on the magnetisation state and temperature of the magnet to prevent complete demagnetisation. In alternative, a novel concept of electrical machine equipped with variable magnetic force magnets has been presented [8], [9]. Basically, the idea is to exploit two diverse kinds of magnets in the machine: one featuring a high coercive force and one with low coercive force. The magnets that have high coercive force yield constant magnetic flux in the magnetic circuit of the machine, while the magnets that have low coercive force produce a variable magnetic flux depending on the working point of the machine. In this circumstance, it is possible to demagnetise the magnet having low coercive force with a low level of stator current when the machine works at high-speed [8]–[10]. A similar idea has been proposed using the same concept in [11] and [12], referring to a Variable Flux PM Synchronous Machine (VF-PMSM) with series and parallel magnet arrangements, as illustrated in Fig. 1.
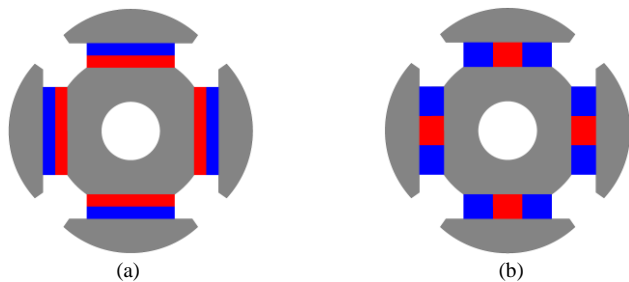
Fig. 1: Concept of Variable Flux PM Synchronous Machine, (a): high (blue) and low (red) coercive force magnets in series, (b): parallel configuration (adopted from [11]).

Fig. 2: Preparing multilayer magnet specimens, (a): hydraulic compression molding machine, (b): sample of a multilayer magnet (b).

This research highlights that both series and parallel configurations of magnets can enhance the torque production capability of the machine, but series configuration demonstrates an improved power capability with respect to the parallel one when the machine operates in high-speed regions. On the basis of the studies presented in literature, it seems that almost all the PM configurations for VF-PMSMs are devoted to electromagnetic actuators with PMs located inside the rotor structure and not directly faced at the air gap (i.e. the interior PM structures) [11], [13]–[15].

With regard to the magnetic structures presented in Fig. 1, the high coercive force magnets or '*strong magnets*' and low coercive force '*weak magnets*' are always separate pieces of magnets glued together. This makes the production and assembling process difficult and expensive. The use of multi-material 3D printing technology, also known as multi-material additive manufacturing, could be an appropriate solution to overcome this issue, but it still seems relatively expensive. Compaction of magnetic materials is an alternative practicable and cost-efficient solution that has been explored recently by the authors. The possibility of simultaneously compressing different soft and hard magnetic powder materials to obtain unified multilayer magnetic blocks has been proved in [16]. In addition, manufacturing approach and characterisation of the self-produced multilayer magnets have been conducted on the basis of experimental measurements taking into account the arrangement of the magnets, considering both parallel and series configuration. The results showed promising magnetic performance in terms of efficiency and flux weakening capability [17]–[20]. In addition, the applicability of multilayer magnet technology for electrical machine application has been investigated in [21]. In this study, the performance of a conventional surface-mounted PM rotor equipped with single- and double-layer magnets has been evaluated. It was revealed that the machine with double-layer magnets shows an improved efficiency and flux weakening capability. This work extends the studied presented [21] on the applicability of novel multilayer magnet technology made of powdered magnetic materials. In detail, the performance of an axial flux machine in which the double-layer magnets are mounted on the rotor disk will be evaluated on the basis of finite-element analyses (FEA) and experimental tests. An axial flux PM machine (AFPM) has been fabricated with different rotor disks equipped with single-layer and double-layer magnets to experimentally investigate the proposed technology.
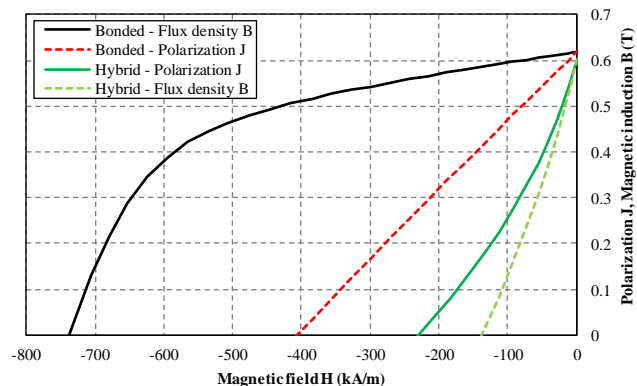

Fig. 3. Measured magnetic characteristics of a bonded and hybrid hard magnetic materials used for building multilayer magnets.

II. MULTILAYER BONDED PERMANENT MAGNETS

Bonded magnets are made of powdered magnetic materials and manufactured through compression, injection, or extrusion molding. The powder material consists of rare earth materials (e.g. NdFeB, SmCo) or hard ferrite and a non-magnetic binder, such as plastic, epoxy or phenolic resins. The magnetic properties of bonded magnets can be adjusted using different binder additives, their percentage and the applied pressure during the fabrication. This unique principle provides an attractive possibility to easily design various grades of the magnet.

Hybrid Magnetic Composite (HMC) materials are a new category of magnets with different magnetic and mechanical characteristics. They consist of hard powdered materials and iron powder with very low oxygen content. These materials are less energetic compared to bonded magnets since they have some per cent of soft magnetic material [22], [23]. More detail on preparation of the materials can be found in [19], [20].

The feasibility of compacting magnetic powders with dissimilar magnetic characteristics in a single block raises the possibility of exploring various combinations of soft and hard magnetic materials to produce the desired multilayer bonded magnet. The authors have exploited their extensive experience to build a unified multilayer magnet block in which the strong PM is made by a conventional bonded magnet, while the weak PM is made by a hybrid magnet. Several samples of multilayer magnets have been built and tested in the laboratory, exploring different material percentages and mixtures. Figure 2 shows the hydraulic press machine employed for the compaction molding process (on the left), and the sample of self-produced multilayer magnets.
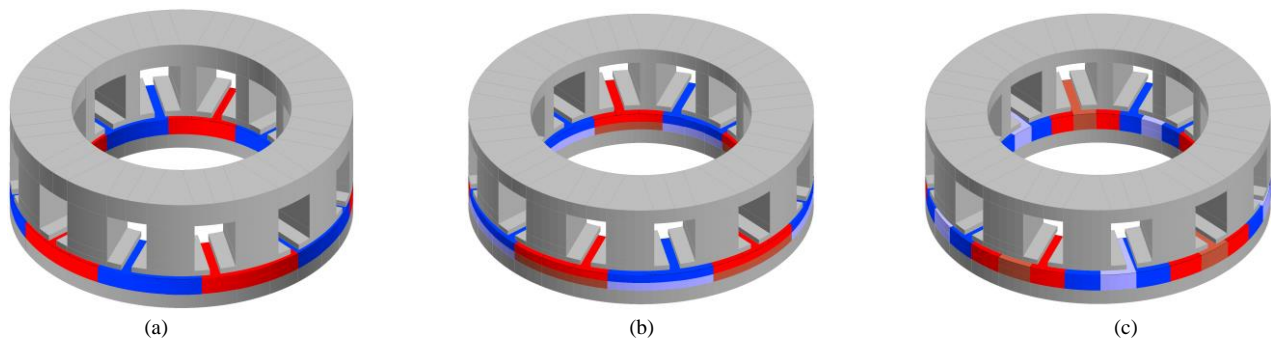
Fig. 4: The structure of the studied AFPM motors, (a): Baseline AFPM machine with single-layer bonded magnets, (b): AFPM machine with double-layer magnet with a series arrangement, (c): AFPM machine with double-layer magnet with a parallel arrangement.

TABLE I
THE MAGNETIC PROPERTIES OF SINGLE-LAYER MAGNETS.

Configuration	Bonded	Hybrid
B_r, (T)	0.617	0.594
H_{CJ}, (kA/m)	738	230
H_{CB}, (kA/m)	406	137
BH_{max}, (kJ/m^3)	64	17

TABLE II
MAIN DATA FOR THE BASELINE MACHINE

Parameter	Value
Inner diameter (mm)	41
Outer diameter (mm)	64
Number of stator slots	12
Number of poles	8
Thickness of stator yoke	4.8
Thickness of rotor disk	3.5
Air gap thickness (mm)	0.8
Slot depth (mm)	10.15
Slot width (mm)	7.76
Number of turns per coil	9
Phase resistance (mΩ)	24.6
Rated speed (rpm)	4000
Rated current (A$_{rms}$)	6
DC bus voltage	12

For the present study, a hybrid magnet with an epoxy resin content of 3.3 % in weight and 50 % in weight of iron have been simultaneously compacted with 3.3 % epoxy resin and neodymium bonded magnet.

Figure 3 shows the induction and polarisation curves of single-layer strong bonded magnet and single-layer weak hybrid magnet accurately measured deploying an available hysteresisgraph. The magnetic properties of the strong (bonded) and weak (hybrid) magnets have been reported in TABLE I

Emphasizing that the magnetic characteristics of multilayer magnets in parallel configurations can be obtained from the single-layer samples. Thus, it is not necessary to characterise the double-layer configurations separately.

III. FINITE ELEMENT MODELLING

To study the applicability of multilayer magnets for electrical machine applications, the geometry of an existing axial-flux PM (AFPM) machine has been taken into consideration as the baseline for the present study. The machine features concentrated tooth windings,12 slots and 8 poles. The rotor is equipped with conventional surface-mounted permanent magnets. The stator is made of SMC, while the rotor disk is made of massive iron. The magnetic properties of the self-produced magnets (bonded and hybrid) have been taken into account for the mounted PMs on the rotor.

The baseline machine has been modelled by means of three-dimensional (3D) FEM simulations using a commercial finite element software. As shown in Fig. 4, the domain regions for the PMs have been subdivided into several parts allowing to model different magnet configurations. With respect to the possible arrangement of the magnets, three models have been taken into consideration: a conventional AFPM machine having single-layer bonded magnets featuring high coercive force (Fig. 4a, the baseline machine), and the AFPM machine equipped with multilayer magnets with series (Fig. 4b) and parallel (Fig. 4c) configurations, respectively.

It should be remarked that the stator and the rotor dimensions and the winding configuration are identical for all the studied machines. The specification of the baseline machine are reported in TABLE II.

In order to have accurate results, the nonlinear characterisation of the self-produced SMC materials and both bonded magnets have been taken into consideration in the FEM models. Once again, it is importance stressing that the nonlinear magnetic characteristics used in the FEM simulations for both soft and hard magnetic materials are obtained by measurements. In addition, the loss behaviour of the SMC materials has been measured and used for all the simulations in this study.

IV. NUMERICAL FEM SIMULATION RESULTS

The electromagnetic performance of the considered AFPM machines equipped with single-layer and multilayer magnets at the rated condition and in flux-weakening operations have been evaluated. The nonlinear transient 3D-FEM simulations have been carried out imposing sinusoidal currents in the stator windings.

A. Flux density distribution

Figure 5 shows the distribution of magnetic flux density of three investigated AFPM machines at no-load conditions. The flux density values in different parts of the machines, namely rotor core B_{cr}, stator yoke B_{ys} and stator teeth B_{ts}, were labelled for analysis.
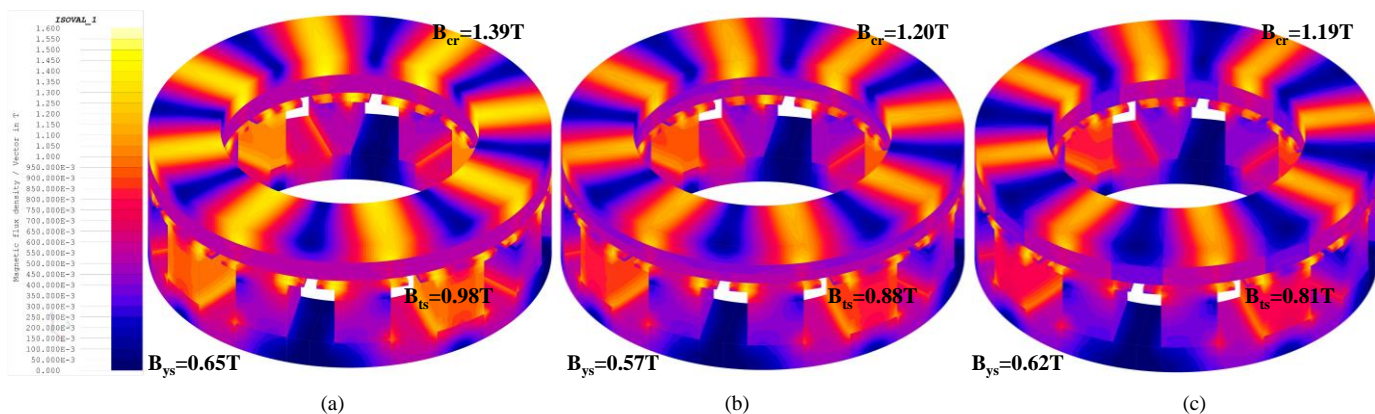
Fig. 5: No-load flux density distribution for the studied machines, (a): baseline AFPM machine with the bonded magnet, (b): AFPM machine with double-layer magnet and series arrangement, (c): AFPM machine with double-layer magnet and parallel arrangement.
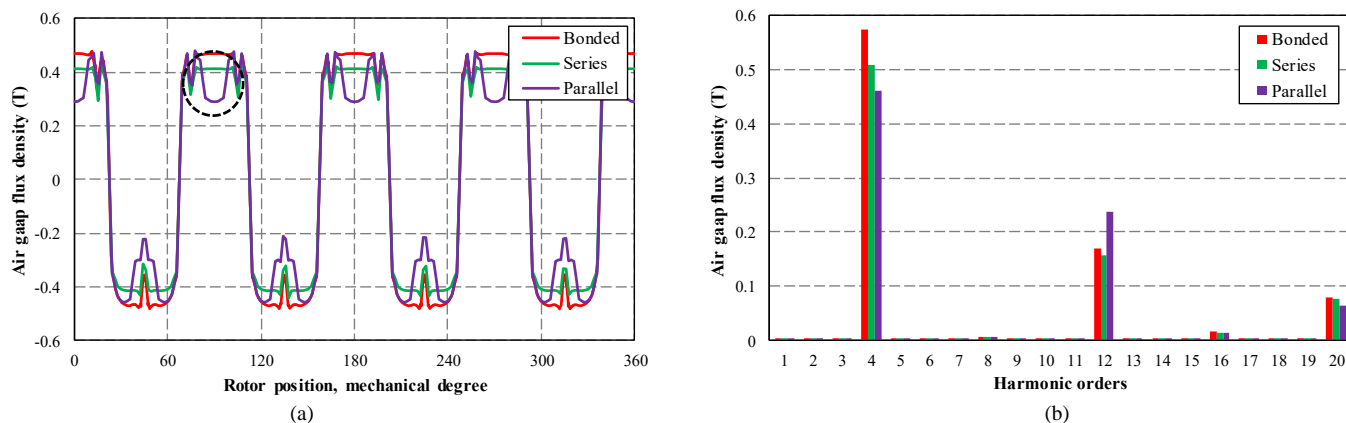

Fig. 6. Comparison of air gap flux density for the studied machine, (a): the waveforms, (b): the harmonic content

Let it be noted that these reported values in Fig. 5 are calculated at average radius of the machines. As can be seen in Fig. 5, baseline AFPM machine equipped with strong bonded magnets exhibits a maximum flux density of approximately 1.4 T in the stator teeth and 1 T in the rotor core. In contrast, the machines equipped with the multilayer magnets feature a lower value of magnetic flux density in their structures due to the weak hybrid PMs. The different magnetic loadings significantly influence on overall performance and efficiency values for the different machines, as articulated in the following sections.

B. Air gap flux density

The waveforms of air gap flux density at the average radius and in the middle of the air gap for the three studied machines as well as their harmonic contents, have been computed and compared in Fig. 6. As expected, the AFPM with bonded PM features the maximum value of the air gap flux density while the AFPM machine with parallel configuration has the minimum value of the air gap flux density. In addition, the waveform of the machine equipped with bonded magnet and the machine with series configuration have the same trend, but their amplitudes are a little different – See Fig. 6a. This variation can be attributed to differences in remanent flux density values. As it can be seen in Fig. 6a, the waveform of air gap flux density for the machines with parallel configuration presents a remarkable drop due to the placing the weak magnet in the middle of this arrangement (the hybrid magnet is sandwiched in between the bonded magnets).

The spectra analysis represented in Fig. 6b highlight the difference among the studied machines. It can be observed that parallel configuration machine introduces the higher value of third harmonics. This third harmonic of air gap flux density leads to higher core losses in the machine. However, it can be utilised in torque production, as reported in [24].

On the other hand, machine employing series configurations exhibit a reduced third harmonic compared to parallel ones. This is because in series layouts, the residual flux value of the magnet faced to the air gap is almost constant for series configurations, while for the parallel ones, it is not.

It is noteworthy mentioning that, although the volume of high coercive force magnet in the series arrangement is lower than that of the parallel ones, the fundamental air gap flux density of the series arrangement is around 10 % higher than the counterpart. This can be attributed to the magnetic shunt effect resulting from the adjacent positioning of the strong and weak PMs. It can be drawn the conclusions that the series configuration can generate more flux in comparison with the parallel configurations.

C. Back Electro-Motive Force (EMF)

The open-circuit back-EMF of the studied machines have been assessed using 3D-FEM at 4000 rpm and shown in Fig. 7. It can be observed that the EMF of machines under study haves the same waveform, and the only difference is the amplitude of induced EMF (See Fig. 7a).
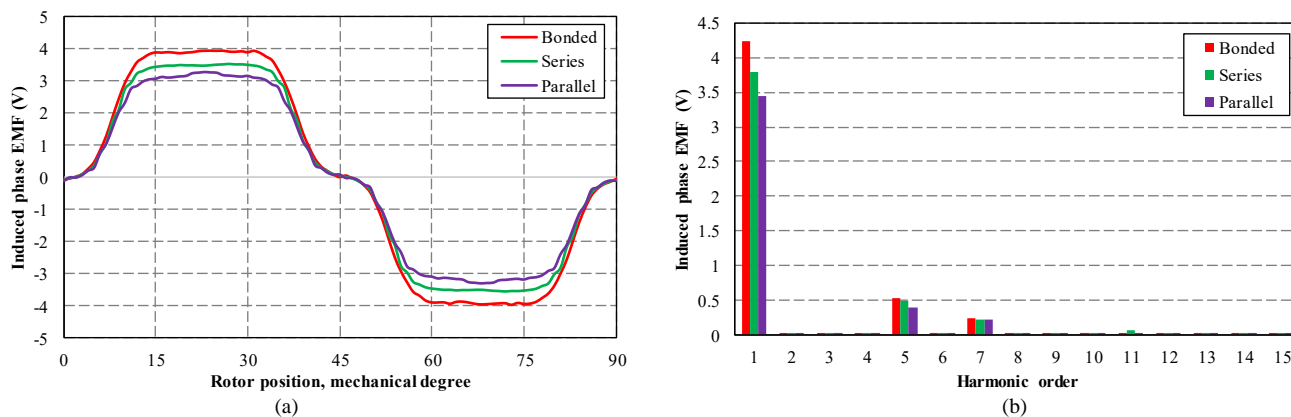
Fig. 7. Comparison of open-circuit back-EMF waveforms at 4000 rpm for the studied machine, (a): the waveforms, (b): harmonic spectra.
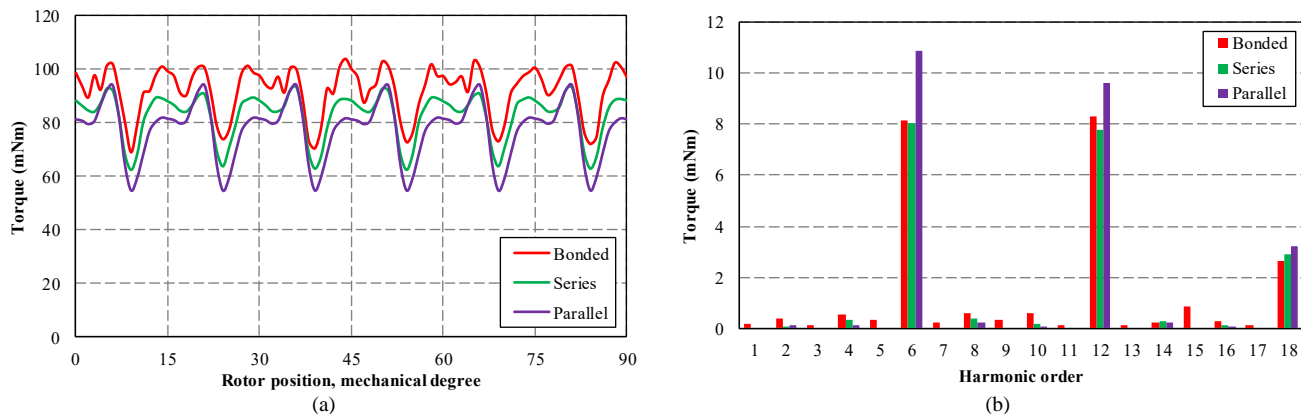

Fig. 8: Comparison of output torque vs. rotor position for the studied motors(a): the torque trend, (b): harmonic spectra.

Noticeably, the machine equipped with just bonded magnet (strong PMs), can provide the maximum value of rms voltage. This is also proved by the harmonic spectra as shown in Fig. 7b. Obviously, the lowest value of induced EMF in the machine with parallel arrangement is due to magnetic shunt effect between adjacent magnets as well as the weak magnets placed in the middle of the magnetic pole.

D. Torque characteristics

The output torque of three studied machines and their Fourier analysis has been evaluated, and the results are shown in Fig. 8. As expected, the baseline machine with strong bonded magnets features the highest torque value. On the other hand, the machines equipped with multilayer magnets with series magnets and parallel ones generate 10 % and 16 % lower torque values compared to the baseline machine, respectively – See TABLE III. In addition, the baseline machine and the machine equipped with the multilayer magnets with series arrangement have comparable torque ripple, around 37 %. However, this value is approximately 14 % higher for the machine with multilayer magnets with parallel configuration – See TABLE III. Obviously, the higher torque ripple of the machines with parallel arrangement multilayer magnet is mainly due to the existence of hybrid magnet layer in the centre of this arrangement as it can be observed from the higher 6th and 12th harmonics of torque. This issue is also highlighted in section IV-B.

Additionally, the cogging torque profiles have been investigated by means of 3D-FEA. As shown in Fig. 9, the cogging torque of the baseline machine with strong bonded magnets and the machine equipped with multilayer magnet with series configuration are almost comparable. On the other side, the AFPM machine equipped with parallel configuration has higher cogging toque value compared to other counterparts.
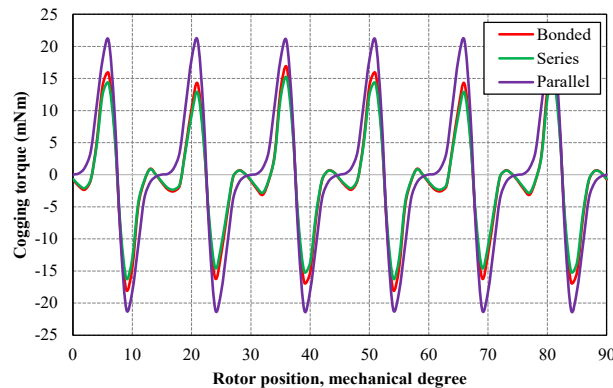

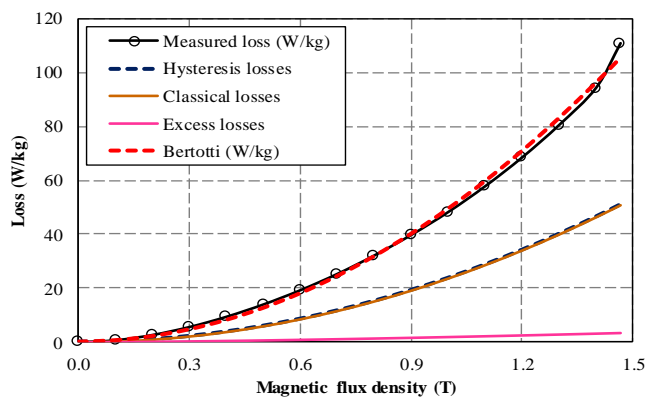Fig. 9: Comparison cogging torque trend for the studied motors.

TABLE III
TORQUE CHARACTERISTICS OF THE STUDIED MACHINES

Configuration	T_{ave} (mNm)	T_{ripple} (%)	$T_{cogging}$ * (mNm)	$T_{reduction}$ (%)
Baseline	92.26	38 %	33.76	baseline
Series	82.84	37 %	31.34	10 %
Parallel	77.63	51 %	42.06	16 %

(*) Peak-to-peak value.

Fig. 10: Iron losses versus magnetic flux density for f = 266.67Hz.

TABLE IV
TORQUE AND POWER DENSITIES FOR THE STUDIED MACHINES

Configuration	Max. Speed[(*)] (rpm)	$T_{density}$ (Nm/dm³)	$P_{density}$ (KW/dm³)	Efficiency (%)
Baseline	5551	0.143	0.0834	64.3%
Series	6326	0.129	0.0853	65.8%
Parallel	7518	0.121	0.0950	63.2%

(*) The base speeds shown in Fig. 12 considered as the maximum speed.

The primary sources of elevated torque ripple and cogging torque originate from the design of the stator and magnet shapes. These issues can be reduced through the careful selection of an appropriate slot / pole combination, as well as the optimisation of both the magnets' shapes and the slot geometry. However, this second-approximation aspect is not the main aim of this study.

E. Losses and efficiency

As previously reported, the machine dimensions and the winding arrangement of the machines taken into consideration in this study are identical. The phase resistance for all the investigated cases is equal to $R_{ph} = 49.2$ mΩ at 25°C. The copper losses in the winding are identical ($P_{Cu} = 2.66$ W) since the peak value of the sinusoidal current flowing in the winding is equal to I = 6 A_{peak} for all the machines. With respect to the small value of copper loss, the values of iron core and mechanical loss components have a substantial impact on the total losses, and therefore the efficiency value.

The iron core losses have been calculated by means of 3D - FEM and on the basis of Bertotti's formula. To precisely calculate the Bertotti's loss coefficients (hysteresis, eddy and excess coefficients), the measured values have been fitted on the loss formula. Figure 10 compares the calculated and measured iron losses versus magnetic flux density. The total losses calculated by means of Bertotti's model well match with the measured values.

It is interesting to observe that the efficiency of the machine with multilayer PM with series configuration has the maximum value while the machine with parallel configuration has the minimum efficiency value. In addition, the power density value of the AFPM machine with the parallel arrangement is around 14 % higher than other ones. Besides, 2 % of output power has been taken into consideration for the mechanical and stray losses.

Moreover, the power density values reported in TABLE IV have been calculated taking into account the different base speed that each machine can attain for a fixed supply voltage. Further details are provided in Section IV.F, where the flux-weakening capabilities for the studied machines are discussed.

The resistivity of the bonded magnet is relatively higher than conventional magnets due to the polymeric binders mixed with the main powder during the manicuring process. The resistivity of the self-produced magnets is around 625 μΩ, and the resultant loss in the PMs is negligible (in the range of milliwatt). Thus, this loss component has not been taken into consideration in this study since the studied machines are smalls.

It should be noted that the temperature has a negative impact on the magnet behaviour, specifically during the demagnetisation state [12]. This could make adjusting the magnetic flux density to a desired value very challenging.

It is crucial to state that the magnetic and loss characteristics of the SMC were acquired through rigorous experimental tests, while the phase resistance was directly measured and incorporated into calculations. This meticulous approach ensures a comprehensive assessment of the factors influencing overall performance. Additionally, the efficiency values presented in TABLE IV were derived from a combination of experimental measurements and simulations.

F. Flux-weakening operation

The fundamental operational principle of variable flux PM machines has been described in Section I. As previously mentioned, the degree of magnetic field strength within the air gap can be dynamically manipulated through the controlled introduction of current pulses into the stator windings [4]–[7]. These controlled pulses of current induce partial demagnetization within the magnets, effectively shifting their operational points. Particularly, the application of this concept is advantageous with low coercive force magnets, as they necessitate significantly lower demagnetization fields. This characteristic enables the possibility of inducing partial or even full demagnetization, and intriguingly magnetizing in the opposite direction, particularly with higher field intensity values. Consequently, this inherent capability allows for adjusting the working point of multilayer magnets, transitioning from maximum remanence to a significantly lower value by applying current pulses of varying amplitudes. This sophisticated technique represents the core of the proposed approach, underscoring its potential in achieving dynamic control and optimization within variable flux PM machines.

Figure 11 shows the supply voltage required to impose the rated i_q stator current for different i_d current values. For higher d-axis current components, lower voltage levels are required to impose the rated i_q current because of the reduced magnetic flux into the machine. This inevitably reflects into the machine flux weakening capabilities with a fixed supply voltage and a fixed current vector. Figure 12 demonstrates the torque–speed curves for the three AFPM machines considered in this study at rated operation condition. It can be seen that employing double-layer magnet technology increases the constant power speed range of the machines.
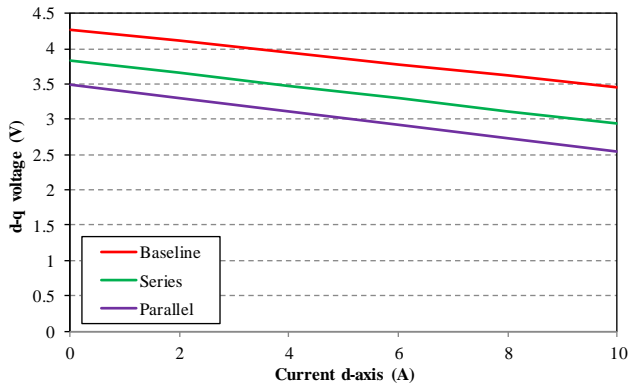
Fig. 11: Voltage vs. negative d-axis current for the studied machines with rated i_q current.
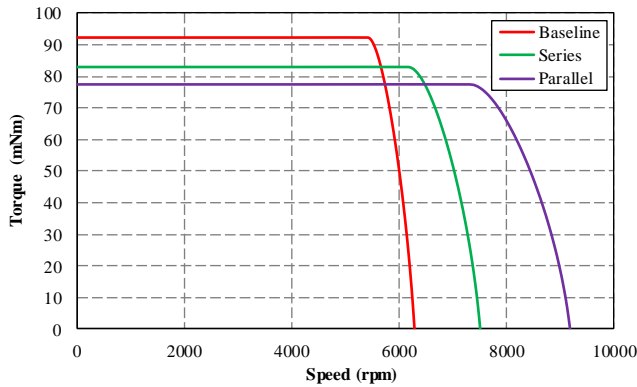

Fig. 12: Torque-speed curves for the single-layer and multilayer magnet machines with the rated stator current of 6 A$_{max}$ (V$_{dc}$ = 12V).

V. MANUFACTURING AND EXPERIMENTAL TESTS

Three axial-flux machines have been manufactured to validate and verify the numerical FEM models: i) AFPM motor with strong bonded magnets, ii) AFPM motor with multilayer magnet with series configuration, iii) AFPM motor with parallel magnet configuration.

The stator together with the winding arrangement of three prototypes are identical, meaning that one stator and three rotor disks equipped with different magnets have been built. In addition, the stator core is made of SMC materials and the rotor core is made of massive iron for all the prototypes.

It is worth mentioning that it was not possible to build the multilayer magnet with parallel configuration due to the facilities available to the authors. However, a prototype with parallel arrangement of strong bonded and weak hybrid magnets glued together has been prepared to have a comprehensive experimental evaluation. Figure 13 shows the test bench, stator and rotor of the manufactured prototypes equipped with multilayer magnets with series arrangement.

Notably, the FEM model of the machine with parallel arrangement has been calibrated based, and the air gap length for this case increased 0.2 mm to maintain the same value of flux per pole with respect to the measurement. The main reason for this difference is due to the manufacturing process, the thickness of glue used during the assembling process. As previously reported, multilayer magnet technology was employed in this case due to the limited facilities and the separate magnet pieces mounted on the rotor.
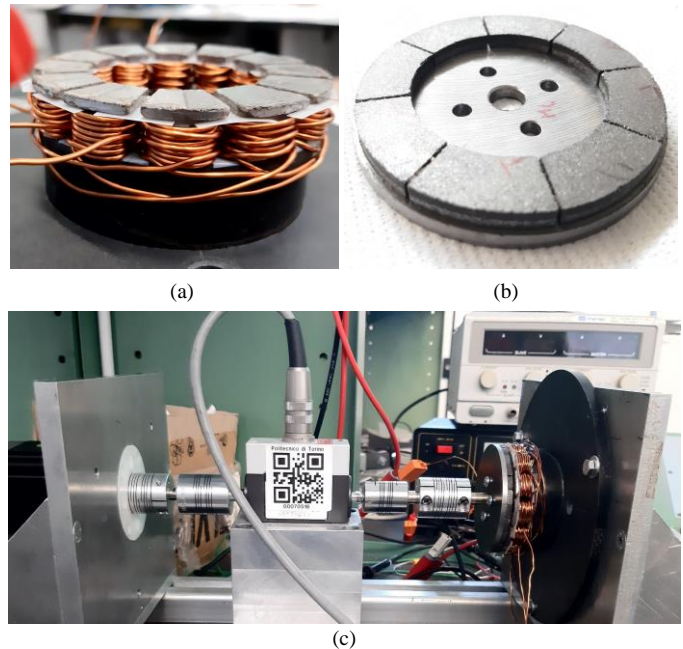

(a)   (b)

(c)

Fig. 13:The built prototype and the test bench used during the measurement: a): stator and windings, (b): the rotor equipped with multilayer magnet with series configuration, c): no-load test bench
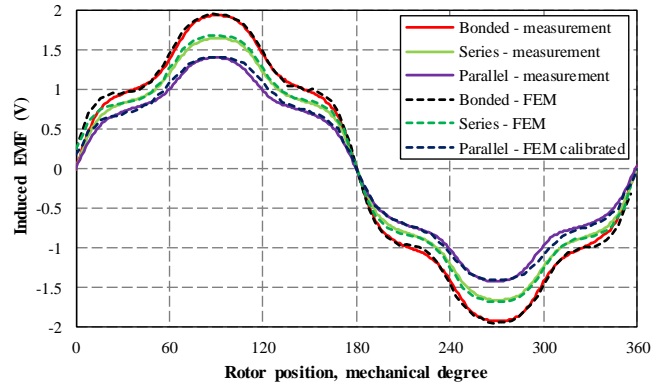
Fig. 14: Comparison of induced line EMF acquired by experimental test and FEM model @ 1000 rpm.

Fig. 15: Comparison of torque values versus various current obtained by experiment and FEM model.

The parasitic gaps between the magnet pieces lead to have lower flux per pole in this case. Since these gaps are very small, it is not possible to measure them experimentally and apply them in the FEM model. For this reason, the air gap length of the machine has been adjusted.

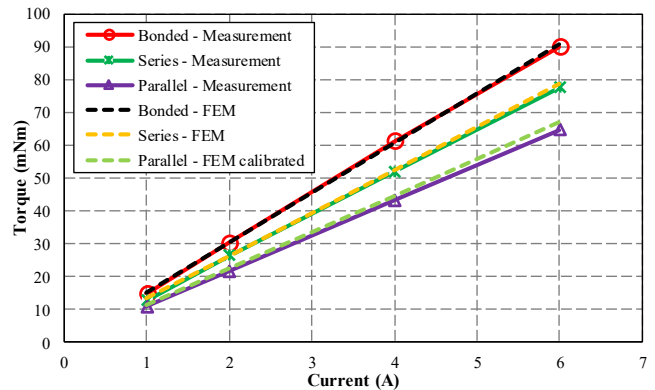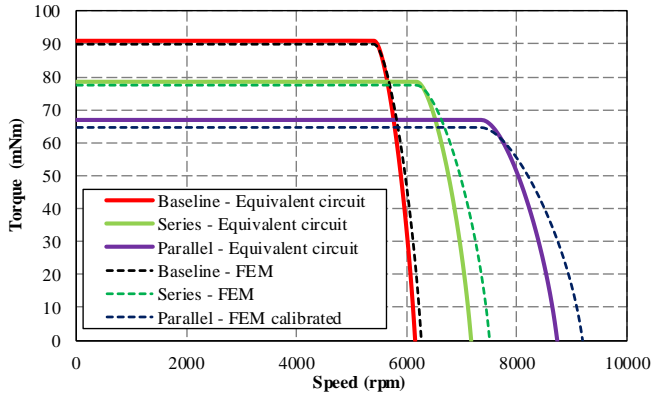Fig. 16: Torque-speed curves computed by the equivalent circuit ($6 A_{max}$, $V_{dc} = 12V$, parameter by measurements and FEM models).

Fig. 17: Torque-speed measurments for three prototyped machines.

Fig. 18: Torque-speed measurments for three prototyped machines.

TABLE V
EQUIVALENT CIRCUIT PARAMETERS OF THE PROTOTYPES
OBTAINED BY MEASUREMENT AND FEM

		Baseline	Series	Parallel
Measurement	R_s (mΩ)		49.20	
	L_s (μH)	31.30	33.21	33.59
	k_E (mV/rad)	7.09	6.20	5.20
	k_T (mNm/A$_{max}$)	15.14	13.11	11.15
FEM	Imposed R_s (mΩ)		49.20	
	L_s (μH)	38.14	47.56	46.99
	k_E (mV/rad)	7.09	6.20	5.20
	k_T (mNm/A$_{max}$)	15.00	12.91	10.76

Extensive measurements have been conducted on the prototypes to verify the FEM models. The predicted FEM results and measured line back-EMF waveforms of three studied machines have been compared as shown in Fig. 14. It can be clearly seen that the waveforms obtained on the basis of numerical models and experimental tests are well matched.

In addition, Fig. 15 compares the variation of shaft torque with the maximum phase current attained by measurements and FEM simulations. It can be observed that there is a very good agreement between the values obtained by the measurements and the values computed by FEM. The equivalent circuit parameters of the prototypes, including winding resistance R_s, inductance L_s, EMF constant k_E and torque constants k_T have been determined by means of experimental measurements and FEM simulations as reported in TABLE V.

The measured and calculated parameters have been employed to compute the torque-speed curves of the machines at the rated operating condition, as shown in Fig. 16.

It can be seen that the maximum speed of the prototypes is slightly different with respect to the FEM models, which is due to the different inductance values. Also, to verify the computed torque-speed curves, some points have been checked by the measurement, as presented in Fig. 17. Furthermore, the efficiency of the examined machines has been evaluated using a hybrid approach that combines measurements and 3D-FEM simulations, as detailed in IV.E. The resulting efficiency values exhibit close alignment with those presented in TABLE IV.
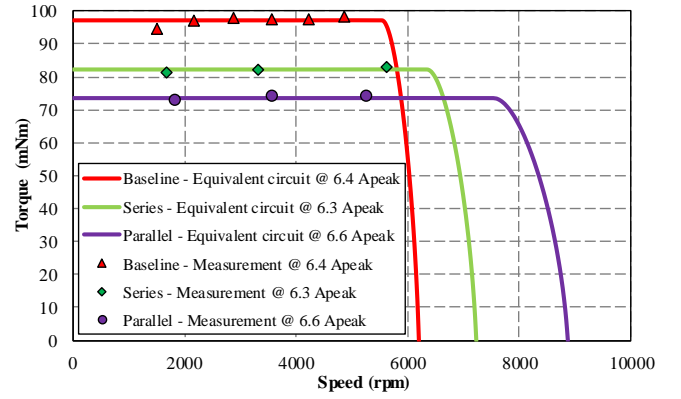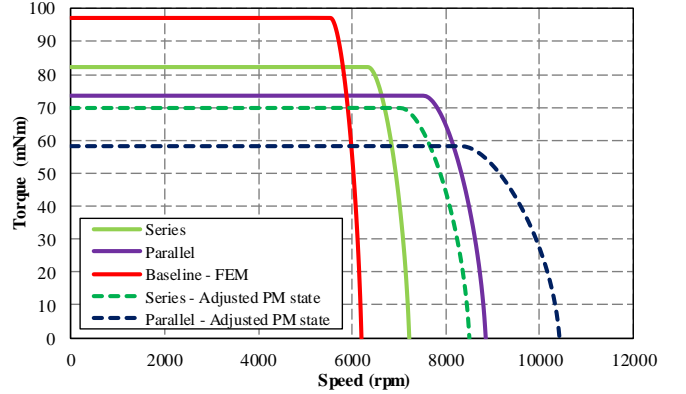
The electromagnetic performance of the proposed machine in larger scales is likely to align with the hypothetical analysis presented in this study. There are some studies available in the literature discussed the scalability of similar machine structure in details [25], [26].

It is important to emphasize that the machines employed multilayer magnets usually require considerably lower current during flux weakening operations. Consequently, the joule losses generated in the windings are minimized. Hence, the dissipation of joule losses is reduced in comparison to machines equipped with strong magnets, which also eliminates potential thermal concerns. A prominent challenge that might arise when dealing with larger multilayer specimens pertains to the manufacturing process, which necessitates high compression forces. Overcoming this challenge would entail further research and development, accompanied by the construction of additional machine prototypes for experimental assessment at various stages.

VI. MAGNETISATION STATE OF MULTILAYER MAGNETS

An adequate control strategy is required to manipulate the value of flux in the air gap. In other words, the spatial distribution of the magnetisation is adjusted to partially demagnetise / remagnetise the magnets. The value of injected pulse current, as well as pulse width, are the critical points for this purpose.

Several studies have already been carried out various control methodologies and discussed the appropriate approach to do that [6], [27], [28]. The presented study mainly focuses on the

applicability of the multilayer magnet technology to prove the concept experimentally, and it does not focus on the control part due to the unavailability of a drive to the authors. For this reason, to investigate the enhancement of flux weakening capability of the machine, the FEM model of the prototypes together with the properties of the materials.

Figure 18 represents torque-speed curves of the studied machines under normal operating points of the machine and after adjusting the magnetisation state of the magnets.

It can be clearly seen a remarkable enhancement in the working speed range of the machines. Generally speaking, the electromagnetic torque in variable flux machines can be calculated by:

$$T_{ele} = 3\left(\frac{P}{2}\right)\{k\lambda_{pm}i_q\} \qquad (1)$$

Where P is the number of poles, λ_{pm} is flux linkage due to the magnets, L_d and L_q are the d- and q-axis inductances, i_d and i_q are the current components in the d- and q-axis, and k is the magnetisation state coefficient which can be obtained for on the basis of the materials proprieties as well as the injected pulse current in negative d-axis direction [6].

VII. Cost Assessment

During the design stage, the final cost of the machine is as important as achieving the highest performance. Obviously, the used materials represent one of the key factors which impact the final cost of the machine, specifically magnets, which are the most expensive elements.
Considering that the volume and weight of the iron core and copper are the same for all the machines under investigation, their final costs are mainly affected by the different types and volume shares of used magnets. Figure 18 compares the cost of the magnets used in each machine structure. Besides the total cost of the magnet, the chart in Fig. 19 also clearly shows the different volume shares between bonded and hybrid PM for the three studied alternatives. The prices of bonded and hybrid materials are considered 60 €/Kg and 30 €/Kg, respectively. This price refers to small quantity purchases for laboratory work and prototypes production. These values are definitely reduced in mass production.

As seen, the cost of the machines equipped with multilayer magnets is approximately 17 – 25 % cheaper than the baseline machine with bonded magnets.
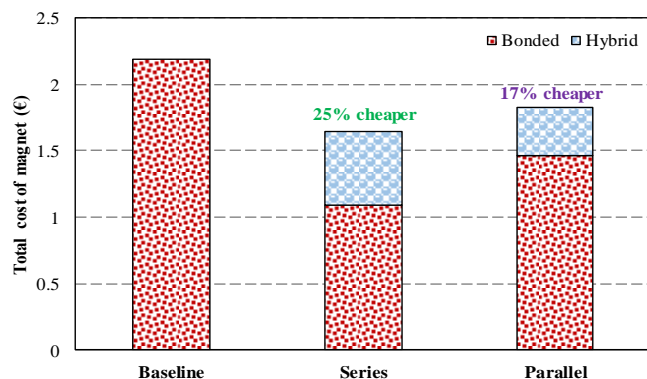

Fig. 19: Comparison the magnet cost in the studied machines.

Also, the cost of multilayer series magnets is less than that of the multilayer parallel magnets. Once again, it has to be highlighted here that 50 % of the weight of the materials used for the production of the hybrid
magnet is pure iron and the rest is NdFeB powder materials and resin. The quantity of the resin used during the preparation of the material plays a prominent role in the density of the hybrid magnet. However, based on the experimental measurements, the density of both bonded and hybrid magnets is comparable, around 5500 kg/m³.

The overall performance of the machine alternatives equipped with multilayer magnets has been investigated and compared with the baseline machine with conventional bonded magnets mounted on the rotor. The obtained results reveal that the multilayer series configurations can provide higher output torque and efficiency than their counterparts. Moreover, the torque density of the machines equipped with multilayer magnets in series arrangement is higher than the one with parallel magnet arrangement. In addition, three prototypes have been manufactured to investigate the proposed idea experimentally.

The measured results prove good reliability of the FEM models. Besides, material cost evaluation has been carried out knowing the volume and weight of materials of each model. It was found that the machine with multilayer magnets with series configurations is 25 % cheaper than the baseline machine with bonded magnets.

VIII. Conclusion

This paper presents a comprehensive study on the application of the proposed multilayer magnet technology for electrical machine applications. An especial focus is paid on investigating various AFPM machines that exploit surface-mounted multilayer magnets consisting of PMs with variable magnetic force. The characterisation of self-produced bonded and hybrid PMs, which have been carefully measured, are utilized for all modelling and analyses.

The comparative analysis is conducted on the basis of numerical FEM simulations, taking into account different machine alternatives. In detail, two potential arrangements, namely parallel and series, are thoroughly investigated in the study. Indeed, the concept of obtaining equivalent magnets by layering two PMs with different coercive force grades holds promise for electrical machine applications, especially when there is a need to balance voltage limits while ensuring acceptable torques at high speeds. This approach allows for tailoring the magnetic properties of the multilayer magnets to suit specific operational requirements, potentially improving overall machine performance. This improvement costs reducing the nominal torque at base speed.

As indicated in this study, the incorporation of multilayer magnet technology into surface-mounted PM machines is associated with specific drawbacks. However, it is crucial to highlight that these challenges come with viable solutions, supported by substantial evidence. An essential consideration in this context is the energy-oriented perspective, with a particular focus on operational expenses. The proposed solution centres around the utilization of pulse current to manipulate the

magnetization state, presenting an innovative approach that contrasts with continuous requirements during flux weakening processes [6], [29]. This approach highlights the potential to notably curtail operational costs, while significantly reducing losses and enhancing efficiency during flux weakening.

While this study has identified limitations in the benefits of adopting multilayer magnet technology in surface-mounted PM machines, it is worth noting that the improvements observed are not negligible. These findings imply that, despite the complexity manufacturing of multilayer magnets, there is potential to derive meaningful gains from their application. Additionally, it is important to note that while the advantages might not be prominently demonstrated in the context of surface-mounted PM machines, alternative machine configurations, like internal PM machines [11], [13]–[15], could yield more substantial benefits from multilayer magnets technology.

Further exploration is required to take the advantages of multilayer magnet technology in electrical machines. This could involve investigating alternative designs, exploring different machine topologies, and considering the utilization of varying grades of hard magnetic materials. Such endeavours might result in more pronounced performance enhancements and could yield more promising results. At the end, the research findings demonstrate the practical feasibility of the multilayer PM concept and its application to special rotating AC electrical machines. The findings from this study drive forward the potential impact of multilayer magnet technology, paving the way for advanced innovations in electrical machine design and performance.

REFERENCES

[1]   R. Schifer and T. A. Lipo, "Core loss in buried magnet permanent magnet synchronous motors," *IEEE Transactions on Energy Conversion*, vol. 4, no. 2, pp. 279–284, Jun. 1989, doi: 10.1109/60.17923.

[2]   S. Hlioui *et al.*, "Hybrid Excited Synchronous Machines," *IEEE Trans Magn*, p. 1, 2021, doi: 10.1109/TMAG.2021.3079228.

[3]   Y. Amara, L. Vido, M. Gabsi, E. Hoang, A. Hamid Ben Ahmed, and M. Lecrivain, "Hybrid Excitation Synchronous Machines: Energy-Efficient Solution for Vehicles Propulsion," *IEEE Trans Veh Technol*, vol. 58, no. 5, pp. 2137–2149, 2009, doi: 10.1109/TVT.2008.2009306.

[4]   V. Ostovic, "Memory motors," *IEEE Industry Applications Magazine*, vol. 9, no. 1, pp. 52–61, Jan. 2003, doi: 10.1109/MIA.2003.1176459.

[5]   H. Yang, H. Zheng, Z. Q. Zhu, H. Lin, S. Lyu, and Z. Pan, "Comparative study of partitioned stator memory machines with series and parallel hybrid PM configurations," *IEEE Trans Magn*, vol. 55, no. 7, pp. 1–8, Jul. 2019, doi: 10.1109/TMAG.2019.2894833.

[6]   R. Jayarajan, N. Fernando, and I. U. Nutkani, "A Review on Variable Flux Machine Technology: Topologies, Control Strategies and Magnetic Materials," *IEEE Access*, vol. 7, pp. 70141–70156, 2019, doi: 10.1109/ACCESS.2019.2918953.

[7]   G. Qiao, M. Wang, F. Liu, Y. Liu, and P. Zheng, "Analysis of Novel Hybrid-PM Variable-Flux PMSMs With Series–Parallel Magnetic Circuits," *IEEE Trans Magn*, vol. 57, no. 2, pp. 1–6, Feb. 2021, doi: 10.1109/TMAG.2020.3013624.

[8]   K. Sakai, K. Yuki, Y. Hashiba, N. Takahashi, and K. Yasui, "Principle of the variable-magnetic-force memory motor," in *2009 International Conference on Electrical Machines and Systems*, IEEE, Nov. 2009, pp. 1–6. doi: 10.1109/ICEMS.2009.5382812.

[9]   M. Ibrahim, L. Masisi, and P. Pillay, "Design of variable flux permanent-magnet machine for reduced inverter rating," *IEEE Trans Ind Appl*, vol. 51, no. 5, pp. 3666–3674, Sep. 2015, doi: 10.1109/TIA.2015.2423661.

[10] K. Sakai, H. Hashimoto, and S. Kuramochi, "Principle of hybrid variable-magnetic-force motors," in *2011 IEEE International Electric Machines & Drives Conference (IEMDC)*, IEEE, May 2011, pp. 53–58. doi: 10.1109/IEMDC.2011.5994656.

[11] A. Athavale, K. Sasaki, B. S. Gagas, T. Kato, and R. D. Lorenz, "Variable Flux Permanent Magnet Synchronous Machine (VF-PMSM) Design Methodologies to Meet Electric Vehicle Traction Requirements with Reduced Losses," *IEEE Trans Ind Appl*, vol. 53, no. 5, pp. 4318–4326, Sep. 2017, doi: 10.1109/TIA.2017.2701340.

[12] B. S. Gagas, K. Sasaki, A. Athavale, T. Kato, and R. D. Lorenz, "Magnet temperature effects on the useful properties of variable flux PM synchronous machines and a mitigating method for magnetization changes," *IEEE Trans Ind Appl*, vol. 53, no. 3, pp. 2189–2199, May 2017, doi: 10.1109/TIA.2017.2674627.

[13] Y. Huang, H. Yang, H. Zheng, H. Lin, and Z. Q. Zhu, "Analysis of flux barrier effect of LCF PM in series hybrid magnet variable flux memory machine," *AIP Adv*, vol. 13, no. 2, Feb. 2023, doi: 10.1063/9.0000611.

[14] Kasper Kvinnesland, "Variable Flux Permanent Magnet Synchronous Machines: Building and Testing Simple Designs with High-Coercivity Magnets," MS Thesis, NTNU, 2018. [Online]. Available: https://ntnuopen.ntnu.no/ntnu-xmlui/handle/11250/2574466

[15] G. Qiao, P. Zheng, M. Wang, F. Liu, and Y. Liu, "Design, modelling and analysis of a hybrid-magnet variable-flux PMSM with variable series-parallel magnetic circuit," *Energy Reports*, vol. 8, pp. 1200–1209, Aug. 2022, doi: 10.1016/j.egyr.2022.02.233.

[16] M. A. Darmani, E. Poskovic, L. Ferraris, and A. Cavagnino, "Multiple Layer Compression of SMC and PM Powdered Materials," in *IECON 2019 - 45th Annual Conference of the IEEE Industrial Electronics Society*, Lisbon, Portugal: IEEE, Oct. 2019, pp. 1216–1221. doi: 10.1109/IECON.2019.8927574.

[17] M. Ahmadi Darmani, E. Poskovic, F. Franchini, L. Ferraris, and A. Cavagnino, "Multiple Layer Magnetic Materials for Variable Flux Permanent Magnet Machines," in *2020 International Conference on Electrical Machines (ICEM)*, IEEE, Aug. 2020, pp. 1662–1668. doi: 10.1109/ICEM49940.2020.9270754.

[18] M. Ahmadi Darmani, E. Poskovic, F. Franchini, L. Ferraris, and A. Cavagnino, "Manufacturing and Characterization of Novel Multilayer Magnets for Electrical Machine Applications," *IEEE Transactions on Energy Conversion*, pp. 1–1, 2022, doi: 10.1109/TEC.2022.3174913.

[19] Mostafa Ahmadi Darmani, "Multiphysics Design of Interior Permanent Magnet Machines and Characterization of Innovative Hard Magnetic Material," (Ph.D. dissertation) Politecnico Di Torino, Turin, 2022. Accessed: Jul. 29, 2023. [Online]. Available: https://iris.polito.it/handle/11583/2971120

[20] M. Ahmadi Darmani *et al.*, "Multiple Layer Magnetic Materials for Variable Flux Permanent Magnet Machines," in *2020 International Conference on Electrical Machines (ICEM)*, IEEE, Aug. 2020, pp. 1662–1668. doi: 10.1109/ICEM49940.2020.9270754.

[21] M. Ahmadi Darmani, E. Poskovic, S. Vaschetto, F. Franchini, L. Ferraris, and A. Cavagnino, "Multilayer Bonded Magnets in Surface-Mounted PM Synchronous Machines," in *2020 IEEE Energy Conversion Congress and Exposition (ECCE)*, IEEE, Oct. 2020, pp. 1052–1059. doi: 10.1109/ECCE44975.2020.9235742.

[22] L. Ferraris, F. Franchini, and E. Poskovic, "Hybrid magnetic composite (HMC) materials for sensor applications," in *2016 IEEE Sensors Applications Symposium (SAS)*, IEEE, Apr. 2016, pp. 1–6. doi: 10.1109/SAS.2016.7479833.

[23] E. Poskovic, L. Ferraris, F. Carosio, F. Franchini, and N. Bianchi, "Overview on bonded magnets realization, characterization and adoption in prototypes," in *IECON 2019 - 45th Annual Conference of the IEEE Industrial Electronics Society*, IEEE, Oct. 2019, pp. 1249–1254. doi: 10.1109/IECON.2019.8927827.

[24] S. Sadeghi and A. H. Isfahani, "Electric Machine With Permanent Magnet Rotor." Google Patents, Apr. 30, 2020.

[25] A. M. EL-Refaie and T. M. Jahns, "Scalability of Surface PM Machines With Concentrated Windings Designed to Achieve Wide Speed Ranges of Constant-Power Operation," *IEEE Transactions on Energy Conversion*, vol. 21, no. 2, pp. 362–369, Jun. 2006, doi: 10.1109/TEC.2006.874221.

[26] A. Athavale, D. Reigosa, K. Akatsu, K. Sakai, and R. D. Lorenz, "Scalability and Key Tradeoffs of Variable Flux PM Machines for EV Traction Motor Systems," in *2018 IEEE Energy Conversion Congress and Exposition (ECCE)*, IEEE, Sep. 2018, pp. 2292–2299. doi: 10.1109/ECCE.2018.8558007.

[27] R. Imamura and R. D. Lorenz, "Stator Winding MMF Analysis for Variable Flux and Variable Magnetization Pattern PMSMs," *IEEE Trans Ind Appl*, vol. 56, no. 3, pp. 2644–2653, May 2020, doi: 10.1109/TIA.2020.2981605.

[28] R. Imamura, T. Wu, and R. D. Lorenz, "Design of variable magnetization pattern machines for dynamic changes in the back EMF waveform," *IEEE Trans Ind Appl*, vol. 55, no. 4, pp. 3469–3478, Jul. 2019, doi: 10.1109/TIA.2019.2903028.

[29] M. Ibrahim, L. Masisi, and P. Pillay, "Design of Variable Flux Permanent-Magnet Machine for Reduced Inverter Rating," *IEEE Trans Ind Appl*, vol. 51, no. 5, pp. 3666–3674, Sep. 2015, doi: 10.1109/TIA.2015.2423661.

Mostafa Ahmadi Darmani received the Ph.D. degree in electrical engineering from Politecnico di Torino, Italy, in 2022. From 2013 to 2018, he worked in as an Electrical Engineer and Consultant in different industries, and as an instructor in training centers. Currently, he is with the Power Electronics Drive Control (PEMC) group at University of Nottingham as a Research Fellow in Electrical Machines. His main research interests include the Multiphysics design and analysis of high-performance electrical machines, and advanced materials for electromechanical energy conversion systems. He is a reviewer for several IEEE Transactions and international journals and conferences.
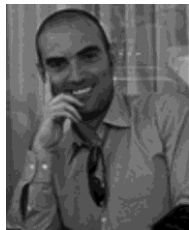
Emir Pošković was born in Sarajevo in Bosnia and Herzegovina, He studied and graduated from the Polytechnic of Turin, where he received B.S. and M.Sc. degree in electrical engineering in 2006 and in 2008, respectively. Also, he received a doctor's degree in electrical energy engineering from the University of Padova in 2020. He is an Assistant Professor with the Energy Department, Politecnico di Torino and a Key Researcher for the Magnetic Characterization Laboratory, Alessandria campus of Politecnico di Torino. His special fields of interest included soft and hard magnetic materials, electrical machines, alternative and renewable energy (micro-hydro, fuel cell, PV-photovoltaic). He has published about 70 scientific papers in conference proceedings and technical journals.

Fausto Franchini received the B.S. degree in electrical engineering from the Politecnico di Torino, Alessandria, Italy, in 2003. Since 2004, he has been a Technician with the Electrical Engineering Laboratory, Politecnico di Torino, where he has been responsible of the laboratory since 2007. His fields of interest include electromagnetic metrology, electromagnetic compatibility, data acquisition, control, and automation.

Luca Ferraris received the M.S. degree in electrical engineering from the Politecnico di Torino, Turin, Italy, in 1992. In 1995, he joined the Department of Electrical Engineering, Politecnico di Torino, where he is currently an Associate Professor of Electrical Machines and Drives and currently coordinates the experimental activities of the Electric and Electromagnetic Laboratories. He has published more than 120 technical papers in conference proceedings and technical journals. His research interests are the energetic behavior of machines, innovative magnetic materials for electromagnetic devices, electrical traction, electromagnetic compatibility, and renewable energies.

Andrea Cavagnino (M'04–SM'10–F'20) was born in Asti, Italy, in 1970. He received his M.Sc. and Ph.D. degrees in electrical engineering from the Politecnico di Torino, Italy, in 1995 and 2000, respectively. He is a professor at the Politecnico di Torino. He has authored or co-authored more than 260 papers, receiving four Best Paper Awards. His research interests include electromagnetic design, thermal design, and energetic behavior of electrical machines. He usually cooperates with factories for a direct technological transfer, and he has been involved in several public and private research projects. Prof. Cavagnino is an Associate Editor of the IEEE Transactions on Energy Conversion (TEC), a Past Chair of the Electrical Machines Technical Committee of the IEEE Industrial Electronics Society, a past Associate Editor of the IEEE Transactions on Industrial Electronics (TIE), and the IEEE Transactions on Industry Applications. He was also a Guest Editor of six Special Sections for IEEE-TIE and co-Editor in Chief of a Special Issue for IEEE-TEC. Prof. Cavagnino was a technical program chair of the IEEE-IEMDC 2015, IEEE-ECCE 2022 and IEEE-ECCE 2025 conferences. He is a reviewer for several IEEE Transactions and other international journals and conferences.

Christopher Gerada (SM'12) is an Associate Pro-Vice-Chancellor for Industrial Strategy and Impact and Full Professor of Electrical Machines. His principal research interest lies in electromagnetic energy conversion in electrical machines and drives, focusing mainly on transport electrification. He has secured over £20M of funding through major industrial, European and UK grants and authored more than 350 referred publications. He received the Ph.D. degree in numerical modelling of electrical machines from The University of Nottingham, Nottingham, U.K., in 2005. He subsequently worked as a Researcher with The University of Nottingham on high-performance electrical drives and on the design and modelling of electromagnetic actuators for aerospace applications. Since 2013, as a Professor at The University of Nottingham. He was awarded a Research Chair from the Royal Academy of Engineering in 2013